PAPER

The topography of metabolic deficits in posterior cortical atrophy (the visual variant of Alzheimer's disease) with FDG-PET

P J Nestor, D Caine, T D Fryer, J Clarke, J R Hodges

J Neurol Neurosurg Psychiatry 2003;**74**:1521–1529

See end of article for authors' affiliations

Correspondence to: Professor John R Hodges, MRC Cognition and Brain Sciences Unit, 15 Chaucer Rd, Cambridge CB2 2EF, UK; john.hodges@mrc-cbu.cam.ac.uk

Received 11 October 2002
In revised form
5 February 2003
Accepted
10 February 2003

Background: The term ''posterior cortical atrophy'' (PCA) refers to a clinical syndrome in which higher order visual processing is disrupted owing to a neurodegenerative disorder, the most commonly associated pathology being Alzheimer's disease.
Objective: To map the topography of hypometabolic brain regions in a group of subjects with PCA who had undergone detailed neuropsychological characterisation.
Methods: Resting cerebral metabolism was measured with (^{18}F)fluorodeoxyglucose-positron emission tomography (FDG-PET) in patients with PCA (n = 6), typical Alzheimer's disease (n = 10), and healthy controls (n = 10). The data were analysed using statistical parametric mapping (SPM99) and region of interest techniques.
Results: Clinically, the PCA subjects showed predominant visuospatial deficits (including features of Balint's syndrome) consistent with damage to the dorsal stream of visual processing. Compared with the controls, the PCA group showed marked glucose hypometabolism primarily affecting the posterior cerebral hemispheres (right worse than left). In addition, the PCA group showed two symmetrical areas of hypometabolism in the region of the frontal eye fields. Compared with typical Alzheimer's disease, the PCA group had selective hypometabolism in the occipito-parietal region (right much worse than left).
Conclusions: The neuropsychological and PET findings are consistent with damage predominantly to the dorsal stream of visual processing. Frontal eye field hypometabolism secondary to loss of input from the occipito-parietal region may be the mechanism for the ocular apraxia seen in Balint's syndrome.

The term posterior cortical atrophy (PCA) was first coined by Benson and colleagues to describe a clinical syndrome in which the onset of a progressive dementia is characterised by the development of higher order visual deficits.[1] By far the most frequent pathological diagnosis in case reports and series is Alzheimer's disease.[2–12] Dementia with Lewy bodies is a common neurodegenerative disorder that also presents with early visuoperceptual deficits but differs from PCA both neurologically (by the emergence of Parkinsonism[13]) and neuropsychologically (by prominent early deficits of attention and executive function.[14]) Creutzfeldt–Jakob pathology has been reported with a presentation of higher order visual failure[10]; however, the rapidly progressive nature of that disease generally leads to a high index of clinical suspicion. Finally, one case of PCA was subsequently shown to have subcortical gliosis,[10] similar to that seen in the frontal and anterior temporal cortices of some cases of fronto-temporal dementia.

Many cases studied pathologically have not undergone rigorous neuropsychological evaluation in life. Yet from those that have there does appear to be evidence that, within the rubric of PCA, cases can be further divided according to the model in which visual information separates into an occipito-parietal pathway (dorsal stream) and an occipito-temporal pathway (ventral stream). The dorsal stream deals preferentially with spatial (''where'') information, while the ventral stream deals preferentially with object identification (''what'') information.[15] The majority of case reports of PCA have described what would appear to be dorsal stream variants with prominent spatial disturbance and, in particular, features of Balint's syndrome; accordingly, most pathological studies have shown that the occipito-parietal region bears the greatest burden of pathology. Ventral stream case reports presenting with visual object agnosia and prosopagnosia have also been described with Alzheimer pathology in the occipito-temporal regions (for example, Hof and Bouras[16]), though from the number of reported cases this would appear to be a less common syndrome. In addition, given that deficits in recognition of objects and faces are seen in semantic dementia,[17] it may be prudent to consider ventral stream cases as having a greater likelihood of including examples of non-Alzheimer pathology.

Case studies combining detailed neuropsychological and neuropathological data inevitably suffer from the long latency between clinical and necropsy evaluation, leading researchers to make assumptions about their relations. Functional brain imaging using (^{18}F)-2-fluoro-deoxy-D-glucose positron emission tomography (FDG-PET) offers a method of studying brain/behaviour relations at the time of neuropsychological assessment. Previous FDG-PET studies of patients with PCA—or at least Alzheimer's disease with prominent visuospatial disturbances—have shown hypometabolism of the parietal regions.[18–21] In most studies, however, the metabolic deficits measured by PET could not be analysed systematically, either because of the single case format or because of technical limitations at the time the studies were done. The largest FDG-PET group study of PCA, using a

Abbreviations: BA, Brodmann area; CMRglc, cerebral metabolic rate for glucose; FDG, (18F)fluorodeoxyglucose; MMSE, mini-mental state examination; MNI, Montreal Neurological Institute; nCMRglc, normalised cerebral metabolic rate for glucose; OMA, oculomotor area; PCA, posterior cortical atrophy; PET, positron emission tomography; ROI, region of interest; SPM, statistical parametric mapping; VOSP, visual object and space perception battery

"region of interest" method, reported significant and symmetrical reductions in glucose metabolism in the occipital association, calcarine, and parietal regions; significantly higher metabolic rates were observed in frontal, anterior cingulate, and inferior and medial temporal regions when contrasted with a group with typical Alzheimer's disease.[22]

The region of interest method, however, cannot systematically survey the entire brain. Our aim in the present study was therefore to examine the whole brain FDG-PET profile of PCA in a group design using the technique of statistical parametric mapping (SPM), in comparison with both healthy controls and, particularly, a group of subjects with typical Alzheimer's disease. The only previous study of PCA using statistical parametric mapping was incomplete in that the whole brain was not included in the field of view.[23] In addition, we conducted a limited region of interest study to assess the reductions in glucose metabolism in absolute terms.

METHODS

Subjects

Patients were recruited from the memory clinic at Addenbrooke's Hospital, Cambridge. Written informed consent was obtained from all the patients (and where necessary from their carers) and from control volunteers, after detailed explanation of the procedures involved. The study had the approval of the local regional ethics committee and the Administration of Radioactive Substances Advisory Committee (ARSAC), UK.

The PCA subjects were defined by the presence of visuospatial deficits as their most prominent presenting symptom, and with visuospatial function as the most severely affected cognitive domain on neuropsychological examination. We excluded subjects presenting with prominent visuospatial deficits who had any of the three proposed "core" features for dementia with Lewy bodies[13] (that is, fluctuating cognitive function with periods of decreased alertness; persistent well formed visual hallucinations; and spontaneous motor features of parkinsonism). In addition, no evidence of any alternative neurological explanation for their symptoms and signs was apparent from clinical assessment or structural neuroimaging, and no subject had a history of ocular disease.

Nine patients with PCA were identified, but three were unable to complete the scanning protocol owing to claustrophobia. This left a group of six PCA subjects for the PET study, all of whom remain under review; at the time of writing the shortest clinical history was more than four years. None has subsequently developed extrapyramidal signs, visual hallucinations, or fluctuations to suggest a diagnosis of dementia with Lewy bodies.

All PCA patients reported an insidious onset of symptoms that typically included misreaching for objects, difficulty in judging distance and motion (such as stepping into oncoming traffic), and colliding with furniture. Difficulty in reading (especially an inability to saccade from the end of one line to the beginning of the next) and in navigating complex environments were common.

On clinical testing, all had gross visuospatial deficits, with some features of Balint's syndrome—an inability to describe complex scenes as a whole (simultanagnosia), difficulty in reaching to visually guided targets (optic ataxia), and difficulty in directing gaze to novel stimuli (ocular apraxia)—were present in most, although only four of the six scanned had all features of the syndrome. When care was taken to ensure that targets were fixated, object recognition appeared relatively preserved. Table 1[t1] shows the presenting complaints and features found on magnetic resonance imaging (MRI) in each of the six subjects.

Mendez and colleagues have recently proposed diagnostic criteria for this syndrome.[24] The core features suggested by these investigators were as follows:

- insidious onset and gradual progression;
- presentation with visual complaints but intact primary visual function;
- evidence of a predominant complex visual disorder on examination;
- proportionally less impairment on tests of memory and verbal fluency;
- relatively preserved insight with or without depression.

We undertook the present study before publication of these criteria; nevertheless, all cases fulfilled them. While these criteria summarise the key clinical features of PCA, their value for defining cases with the syndrome for either clinical or research purposes is questionable. In their proposal, the authors made no mention of dementia with Lewy bodies, even though this is probably the principal differential diagnosis of a degenerative process with prominent visuospatial symptoms and signs.

Ten subjects with typical Alzheimer's disease who fulfilled the NINCDS-ADRDA criteria for probable Alzheimer's disease were also studied.[25] All 10 presented primarily with an amnesic syndrome but with evidence of underfunctioning in at least one other cognitive domain (attention, visuospatial function, language/semantics, executive function) on detailed neuropsychological testing.

Ten aged matched healthy controls were either spouses of the patients or were recruited from local community groups. Controls were screened by a neurologist to ensure that there was no evidence of memory impairment, dementia, or other neurological or major psychiatric illness. The demographic characteristics of the three groups are summarised in table 2[t2]. The Alzheimer's disease and PCA subjects were matched for duration of symptoms and mini-mental state examination (MMSE) score.[26] There was a statistically significant difference, in favour of the PCA group, in years of formal education between the PCA and the Alzheimer's disease groups (unpaired two tailed t test, $p = 0.04$).

Neurological and neuropsychological assessments

Deficits in all the subjects were assessed clinically by a neurologist. Five of the PCA subjects also underwent formal ophthalmological testing. Subjects with typical Alzheimer's disease and PCA underwent a battery of neuropsychological tests including tests of attention (digit span), episodic memory (story recall[27]), language and semantics (category fluency, pyramids and palm trees test,[28] and picture naming[29]), executive function (FAS fluency), and visuospatial function (visual object and space perception battery (VOSP)[30] and Rey figure[31]). With the exception of the visuospatial domain, the selected tests were biased towards those with little or no visual component to minimise the likelihood that a visuospatial deficit confounded the test performance.

Imaging protocol

All subjects were studied using an identical protocol on scanners in the Wolfson Brain Imaging Centre, University of Cambridge. Each subject underwent T1 weighted, three dimensional, spoiled gradient echo sequence (SPGR) volumetric MRI (echo time 5 ms, recovery time 19.1 ms) on a 3Tesla Bruker system for co-registration to PET. The field of view was 25.6×22.0×18.0 cm with a matrix size of 256×256×256. PET scans were done on a General Electric Advance system in three dimensional mode, voxel size 2.35×2.35×4.5 mm, with a field of view of 30×30×15.3 cm.

Table 1 Presenting complaines and magnetic resonance imaging findings in six patients with posterior cortical atrophy

Subject	Sex	Age (years)	Symptom duration (years)	MMSE	Description of presenting complaint	MRI
HM	F	78	10	24	Unable to find objects in a room then they would ''suddenly pop-up''; difficulty getting arms into sleeves of clothes; when reading ''could only see a small part of the page at a time''; misreaching for objects	Widening of Sylvian fissures, mild to moderate parietal atrophy
PG	M	59	3	27	Difficulty reading maps; difficulty navigating in streets; when intending to drive would climb into the back seat of the car; poor concentration and arithmetic skills; memory complaints.	Normal
RH	M	63	6	15	Unable to stay in lane when driving; misjudging distances; unable to dress; when reading could not change from the end of one line to the beginning of the next; unable to insert electrical plugs into sockets.	Moderate generalised atrophy
SK	F	66	3	26	Difficulty with the ''left field of vision''; repeated collisions with the kerb when driving and smashing the left wing mirror; unable to judge distance when hanging out laundry or placing objects in cupboards	Moderate biparietal atrophy
PM	F	58	7	17	Unable to read; poor writing and typing; unable to fasten buttons; unable to find bathroom during the night; poor memory for recent events	Mild to moderate generalised atrophy
AN	M	58	5	18	Colliding with objects on the left; difficulty with navigation; difficulty dressing.	Moderate biparietal atrophy

Age, duration of symptoms, MMSE, and MRI findings are taken from the time of PET scanning.
MMSE, mini-mental state examination; MRI, magnetic resonance imaging; PET, positron emission tomography.

Before the PET scan, subjects fasted for a minimum of eight hours; 30 minutes before isotope injection a radial arterial cannula was inserted for glucose and radioactivity measurements, and a venous cannula for fluorodeoxyglucose (FDG) injection. The subjects were then positioned in a plastic head cradle. Ear plugs and blindfolds were not used, but all subjects were scanned under the same conditions in a dimly lit, quiet room. A 10 minute transmission scan was done for attenuation correction using rotating $^{68}Ge/^{68}Ga$ sources, after which the subjects received an injection of 74 MBq (2 mCi) of FDG over 30 to 60 seconds. PET images were then acquired from t+35 to +55 minutes postinjection, while 14 arterial blood samples were taken over the 55 minute postinjection period to define the FDG input function. Images were reconstructed using the PROMIS algorithm,[32] with corrections applied for attenuation, dead time, scatter, and random coincidences. Cerebral metabolic rate for glucose (CMRglc) was calculated from the image and blood data using the Huang autoradiographic technique.[33]

Image analysis

Image analysis was done on a Sun Microsystems ultrasparc 60 workstation. To minimise normal intersubject variability of resting brain metabolism, PET scans were normalised to the CMRglc of the cerebellar vermis (nCMRglc). This region is thought primarily to reflect intersubject differences in brain metabolism[34] and has been used in similar PET studies of Alzheimer's disease.[35] The remaining stages of the image processing and statistical analysis were done with SPM99 (Wellcome Department of Cognitive Neurology, London) and Matlab5.2 software (Mathworks Inc, Natick, Massachusetts, USA). The PET scans were co-registered to each individual's volumetric MRI and then spatially normalised to the T1-MR template in SPM99 (based on the standard brain of the Montreal Neurological Institute (MNI)). Finally, to minimise effects of interindividual variation in sulcal pattern, the normalised scans were smoothed with a 16 mm full width at half maximum (FWHM) Gaussian filter.

Table 2 General demographic features of the study groups

	PCA (n = 6, 3F)	tAD (n = 10, 4F)	Controls (n = 10, 5F)
Age	63.6 (7.8)	68.1 (7.4)	61.3 (7.6)
MMSE (/30)	21.2 (5.1)	22.8 (1.8)	29.6 (0.5)*
Education (years)	13.3 (2.4)	10.7 (1.4)†	11.3 (1.5)
Symptom duration (years)	5.7 (2.7)	4.8 (2.6)	–

Values are mean (SD).
*$p<0.001$ *v* both AD and PCA; †$p=0.04$ *v* PCA.
F, female; MMSE, mini-mental state examination; PCA, posterior cortical atrophy; tAD, typical Alzheimer's disease.

Statistical analysis of PET data with statistical parametric mapping

The data were analysed in two parts. The first analysis, designed to assess the total extent of affected brain regions, contrasted the PCA group with the controls. The second analysis contrasted the PCA group with the Alzheimer's disease group to determine what specific areas of abnormality were present in excess of those in the temporo-parietal association cortex typically found in Alzheimer's disease. The threshold for analysis of voxels was set at >40% of whole brain mean, to ensure that severely hypometabolic regions were not excluded, while minimising edge effects.[35] Statistical analyses were performed at p(corrected) = 0.05 and p(corrected) = 0.1. Localisation of abnormal clusters was undertaken using the co-planar stereotaxic atlas.[36]

Region of interest study

Regions of interest (ROI) were defined for (right and left) frontal pole, precuneus, cuneus, and the cerebellar vermis on a standard template based on the MNI brain. The subject's PET scans were co-registered to their MRI and then spatially normalised to the T1-MRI template in SPM99. The ROI object map was then overlaid and CMRglc calculated for each ROI using the autoradiographic method. As the aim of the ROI study was absolute CMRglc quantification, a three compartment partial volume correction[37] was applied to each region: each subject's MRI was segmented into grey matter, white matter, and cerebrospinal fluid, and these segments were then smoothed to the resolution of PET using a 6 mm FWHM Gaussian filter. From the superposition of the smoothed segments, the PET signal in each voxel can be related to the percentage of grey matter and white matter within the voxel. By assuming that CMRglc for grey and white matter are

constant in the ROI, these two variables can be determined by solving the set of simultaneous equations representing the signal in the voxels. Consequently, a mean CMRglc for the ROI can be calculated which is not erroneously reduced because of CSF contamination. The results for each region were then analysed by one way analysis of variance (ANOVA), and where significant group effects were found, post hoc Scheffé's tests were used. The data were analysed both as absolute regional CMRglc and, to account for normal interindividual differences in brain metabolism, as an index of each subject's cerebellar vermis CMRglc (that is, normalised to vermis, nCMRglc).

RESULTS

Ocular and visual field assessments

None of the six cases had evidence of ocular abnormalities on neurological examination (pupil responses and fundoscopy). Visual acuity could not be measured reliably owing to the difficulty with fixation. Formal visual field testing was attempted in five subjects; the remaining case, and also the most mild, had normal fields on bedside confrontation testing. Of the five assessed formally, three managed to complete Humphrey automated perimetry, each having evidence of a left homonymous hemianopia. One patient had Bjerrum field assessment which showed left hemifield loss from the right eye and left superior quadrant field loss from the left eye. The final case could only be assessed to confrontation and had evidence of a subtle left homonymous hemianopia. In addition to visual field loss, one subject had evidence of left hemispatial somatosensory and auditory neglect on bedside testing.

Neuropsychology

Selected neuropsychological results are shown in table 3[t3]. No significant differences on Mann–Whitney U tests were seen between the Alzheimer's disease and PCA groups on forward or reverse digit span, category fluency, pyramids and palm trees test,[28] a 64 item picture naming test,[29] or letter (FAS) fluency. As a group, the PCA patients performed better on story recall[27] than the Alzheimer group, although this difference did not reach statistical significance (p = 0.07). It should be noted, however, that unlike the Alzheimer's disease subjects, the PCA subjects showed considerable heterogeneity on memory testing, with some performing at a near normal level. Not unexpectedly, the PCA group performed significantly worse on visuospatial tasks, including copying the Rey complex figure[31] and subtests of the visual object and space perception battery.[30]

Statistical parametric mapping

SPM analysis of the metabolic changes in the group with typical Alzheimer's disease contrasted with the controls is shown in fig 1[f1] as a "template" of the characteristic cortical metabolic changes associated with this condition. At p(corrected) = 0.05, there was hypometabolism in the lateral

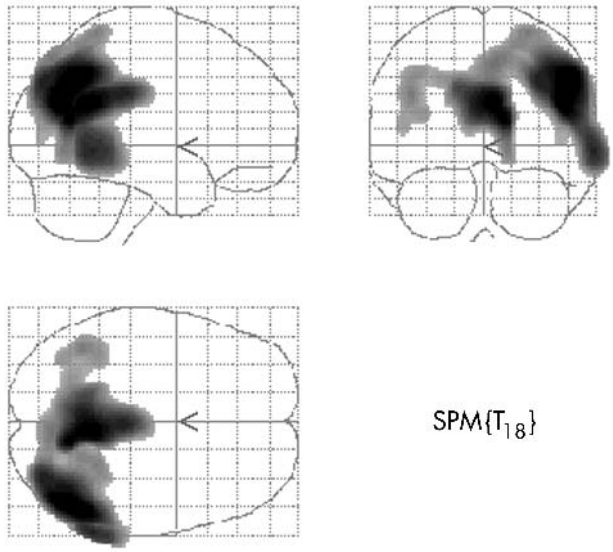

Figure 1 SPM glass brain images of hypometabolic regions in the group with typical Alzheimer's disease compared with the healthy controls at p(corrected) = 0.05. SPM, statistical parametric mapping.

Table 3 Performance on selected neuropsychological tests in the Alzheimer's disease and posterior cortical atrophy groups

	tAD	PCA	Controls (n = 31; age 68.5 (7.2) years)
Attention			
● Forward digit span	6.7 (1.0)	5.7 (1.0)	7.1 (0.9)
● Backward digit span	4.3 (1.7)	3.0 (0.9)	5.4 (1.4)
Memory			
● Logical memory	0.1 (0.3)	1.9 (2.3)	7.8 (3.8)
Language and semantics			
● Category fluency (animals, birds, fruit, dog breeds)	37.3 (12.7)	41.7 (24.2)	60.3 (12.6)
● Pyramids and palm-trees (word version, /52)	50.1 (1.9)	48.3 (4.3)	51.1 (1.1)
● 64 item picture naming (/64)	59.8 (4.1)	56.0 (4.3)	63.8 (0.4)
Visuospatial			
● Rey figure copy (/36)	31.7 (3.8)	1.2 (2.0)†	34.2 (1.6)
Visual object and space perception battery (VOSP)			
● Dot counting (/10)	9.6 (0.5)	4.3 (2.4)†	9.9 (0.3)
● Position discrimination (/20)	NT	11.3 (3.9)	19.8 (0.6)
● Cube analysis (/10)	8.1 (1.6)	2.0 (3.1)*	9.3 (1.5)
● Incomplete letters (/20)	18.6 (1.1)	9.8 (6.9)*	19.2 (0.8)
● Object decision (/20)	17.3 (2.3)	12.7 (5.1)	16.9 (0.8)
Executive			
● Letter fluency (FAS)	38.4 (14.9)	32.8 (20.5)	41.1 (11.6)

Values are mean (SD).
Control scores were obtained from the control panel of the Cognition and Brain Sciences Unit, Cambridge.
*p<0.05, †p<0.005 *v* tAD.
FAS, ; NT, not tested; PCA, posterior cortical atrophy; tAD, typical Alzheimer's disease.

temporo-parietal association cortex (right worse than left), as well as involvement of the posterior cingulate and precuneus. At p(corrected) = 0.1, additional abnormal regions in left frontal pole and left dorsolateral prefrontal cortex were seen (data not shown).

Comparison of PCA with controls (fig 2[f2]) at p(corrected) = 0.05 revealed extensive abnormalities in the posterior hemispheres (occipito-parieto-temporal regions). Although bilateral in distribution, the changes were more severe on the right. In addition, there were two localised areas of abnormality in the dorsolateral frontal lobes. These areas were approximately symmetrical and extended from Brodmann area (BA) 6/8 to 8/9 (Talairach coordinates: right, $x = 30$, $y = 27$, $z = 37$ to $x = 33$, $y = 0$, $z = 47$; left, $x = -22$, $y = 21$, $z = 47$ to $x = -31$, $y = 4$, $z = 49$), approximating the area of the frontal eye fields (fig 3[f3]). Two small regions slightly rostral to these areas were also identified (BA 9), but otherwise the frontal lobes were spared, as were the anterior temporal lobes. At p(corrected) = 0.1, the profile was similar, although the frontal abnormalities were slightly more extensive. At this significance threshold, in the coronal plane the frontal eye field clusters extended from $y = -4$ to $y = +30$ (bilateral; data not shown). These clusters were also considered in terms of gyral anatomy by projecting them onto spatially normalised MRI scans. Using this method, the cluster ran along the fundus of the caudal part of the superior frontal sulcus (fig 3[f3]).

The contrast of PCA with typical Alzheimer's disease (fig 4[f4]) yielded much more localised areas of hypometabolism in the PCA group. At p(corrected) = 0.05, the hypometabolic region was almost exclusively right sided and extended from the primary visual cortex (BA 17; $x = 14$, $y = -94$, $z = -2$) through the dorsal visual association cortex (dorsal BA 18/19) to the parietal lobe (BA 7/40; $x = 22$, $y = -52$, $z = 66$ to $x = 54$, $y = -28$, $z = 28$), with maximum reduction in metabolism in the region of the occipito-parietal junction (BA19/7; $x = 34$, $y = -70$, $z = 38$). At p(corrected) = 0.1, the right sided abnormality was similar but there was also evidence of involvement of the left hemisphere: two discrete regions were identified in the medial occipital gyrus (BA 18; $x = -34$, $y = -86$, $z = 10$) and parietal lobe (BA7; $x = -22$, $y = -42$, $z = 40$) (data not shown).

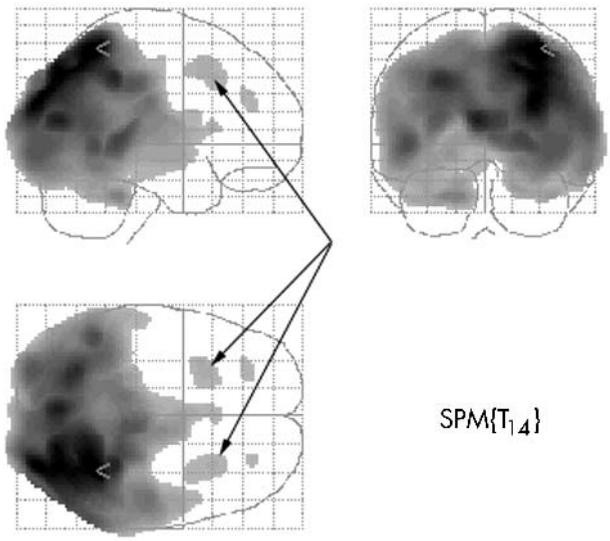

Figure 2 SPM glass brain images of hypometabolic regions in the group with posterior cortical atrophy compared with the healthy controls at p(corrected) = 0.05. Arrows indicate hypometabolic areas corresponding to BA 6/8 (frontal eye fields). SPM, statistical parametric mapping.

Figure 3 Sectioned coronal image of the contrast between posterior cortical atrophy and control at p(corrected) = 0.05. The image is at y+14 mm and shows symmetrical areas of hypometabolism in the region of the frontal eye fields.

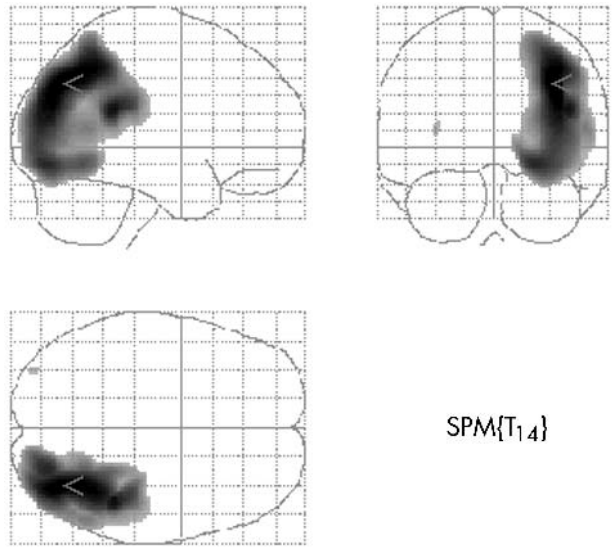

Figure 4 SPM glass brain images of hypometabolic regions in posterior cortical atrophy compared with typical Alzheimer's disease at p(corrected) = 0.05. SPM, statistical parametric mapping.

Of note, the statistical difference in nCMRglc of the posterior cingulate/precuneus seen when PCA was contrasted with controls was not seen when PCA was contrasted with Alzheimer's disease (compare figs 1[f1], 2[f2], and 4[f4]), suggesting a comparable degree of reduction in nCMRglc in this region between PCA and Alzheimer's disease. In addition, the hypometabolic regions in the frontal eye fields were not seen in the contrast of PCA with typical Alzheimer's disease; however, they were present when the data were analysed at the less rigorous threshold of p(uncorrected) = 0.001 (data not shown). Table 4[t4] summarises the Talairach coordinates for statistical maxima within clusters and their corresponding approximate brain locations at p(corrected) = 0.05 for the contrasts of PCA from controls and PCA from typical Alzheimer's disease.

Table 4 Summary of Talairach coordinates at p(corrected) = 0.05 in PCA minus controls and PCA minus tAD comparisons

Cluster size (K_E)	p Value (corrected)	*t*	Coordinates *x, y, z* (mm)	Location
PCA minus controls				
62802	0.000	14.93	34, −52, 58	R superior parietal lobule (BA 7)
	0.000	14.59	30, −88, 26	R superior/medial occipital gyrus (dorsal BA 18/19)
	0.000	14.59	30, −74, 42	R superior parietal lobule (BA 7)
224	0.017	7.08	−28, 12, 46	L superior/medial frontal gyrus (BA 6/8)
358	0.024	6.82	30, 18, 42	R medial frontal gyrus (BA 6/8)
	0.030	6.62	34, 8, 46	R medial frontal gyrus (BA 6/8)
64	0.032	6.56	−28, 40, 28	L medial frontal gyrus (BA 9)
35	0.037	6.44	26, 42, 24	R medial frontal gyrus (BA 9)
PCA minus tAD				
10776	0.002	9.01	34, −70, 38	R superior parietal lobule (BA 7/19)
	0.002	8.92	34, −62, 42	R superior parietal lobule (BA 7)
	0.003	8.56	44, −40, 22	R inferior parietal lobule (BA 40)
11	0.045	6.13	−34, −86, 10	L medial occipital gyrus (BA 18)

L, left; PCA, posterior cortical atrophy; R, right; tAD, typical Alzheimer's disease.

Region of interest analysis

The results of the ROI study are illustrated in fig 5[f5]. One way analysis of variance (ANOVA) of the regional CMRglc values showed significant group effects (df = 2,23) for left frontal pole ($F = 4.3$, $p = 0.03$), right precuneus ($F = 22.1$, $p<0.0001$), left precuneus ($F = 17.4$, $p<0.0001$), and right cuneus ($F = 11.3$, $p = 0.0004$), but not right frontal pole ($F = 2.2$, $p = 0.13$) or left cuneus ($F = 1.3$, $p = 0.28$). When

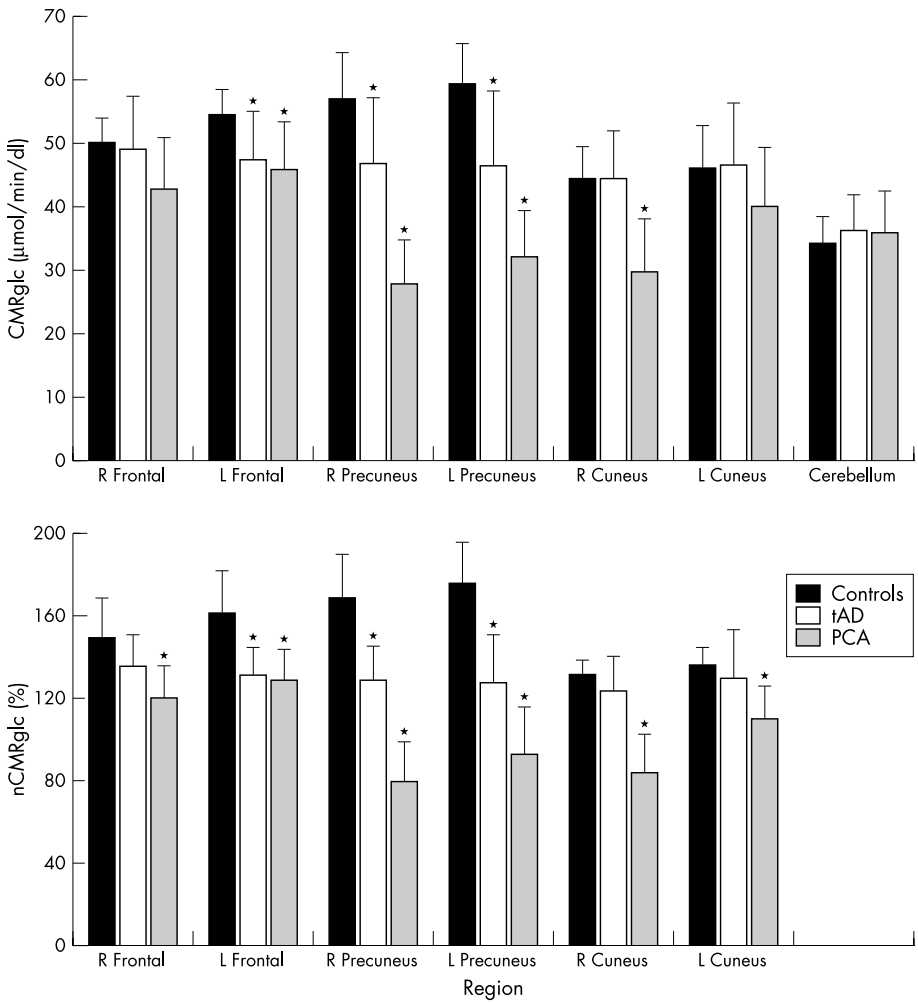

Figure 5 Mean cerebral metabolic rate for glucose (CMRglc) for regions of interest by group (top panel: absolute CMRglc; bottom panel: normalised to cerebellar vermis). Error bars = SD. *Significant reduction from other group(s); see table 5 for details.

Table 5 Summary of p values from post hoc comparisons (Scheffé's tests) in the region of interest study

	R frontal	L frontal	R precuneus	L precuneus	R cuneus	L cuneus
CMRglc						
C *v* tAD		0.080	0.04	0.014	0.99	
C *v* PCA		0.056	<0.0001	<0.0001	0.0011	
tAD *v* PCA		0.88	0.002	0.019	0.0013	
nCMRglc						
C *v* tAD	0.27	0.0025	0.0004	0.0003	0.52	0.74
C *v* PCA	0.013	0.0037	<0.0001	<0.0001	<0.0001	0.038
tAD *v* PCA	0.22	0.93	0.0002	0.017	<0.0001	0.14

C, control; L, left; PCA, posterior cortical atrophy; R, right; tAD, typical Alzheimer's disease.

each subject's data were normalised to the CMRglc of their vermis (nCMRglc), one way ANOVA were significant for all regions: right frontal pole ($F = 5.3$, $p = 0.01$), left frontal pole ($F = 10.5$, $p = 0.0006$), right precuneus ($F = 42.0$, $p<0.0001$), left precuneus ($F = 28.3$, $p<0.0001$), right cuneus ($F = 22.3$, $p<0.0001$), and left cuneus ($F = 3.8$, $p = 0.04$). The post hoc comparisons are presented in table 5[t5]. In summary, reductions in CMRglc when either typical Alzheimer's disease or PCA was contrasted with controls were greatest in the precuneus (bilaterally). In addition, the PCA group showed significantly greater metabolic reductions than typical Alzheimer's disease in right and left precuneus and right cuneus.

DISCUSSION

To our knowledge this is the first study to analyse the topography of hypometabolism in PCA over the whole brain, and to contrast this directly with the changes in typical Alzheimer's disease using a voxel based image analysis method. Clinically, the PCA group showed similar performance on non-visuospatial cognitive tasks to the group with mild Alzheimer's disease but all had additional marked impairment on visuospatial tasks. With regard to subtests of the VOSP in PCA, the most significant impairments were for spatial perception tasks (dot counting, cube analysis) compared with object perception (incomplete letters, object decision). The PCA group's performance did not differ significantly from typical Alzheimer's disease on the 64 item picture naming test, which also taps object perception. Some features of Balint's syndrome were present in most cases, and five of the six showed evidence of visual loss in the left hemifield.

Six subjects of the nine recruited completed the imaging study, three dropping out because of claustrophobia. This dropout rate is considerably higher than in other dementia cohorts undergoing the same imaging protocol and may not be a chance finding. The three cases who did not tolerate scanning also reported the development of new onset claustrophobic symptoms (such as in elevators) over the course of their illness. It may be that the disintegration of a coherent visuospatial representation of extrapersonal space exacerbates, or even gives rise to, such phobic symptoms.

In the following discussion we will focus on the results of the statistical parametric mapping study, but it should be noted that the results were concordant with those of the ROI study in that the PCA group showed greater reductions in CMRglc in the posterior ROIs (precuneus and cuneus) than in the frontal ROI; the right hemisphere was more significantly involved than the left in the PCA group; and more significant hypometabolism was noted in the cuneus in PCA than in typical Alzheimer's disease.

When contrasted with healthy controls, hypometabolism in PCA was found throughout the posterior regions of the cerebral hemispheres. Relative to controls, there was considerable overlap of abnormal regions with those seen in typical Alzheimer's disease, making it difficult to attribute their clinical profile to a specific anatomical substrate. To circumvent this problem, the PCA and Alzheimer's disease groups were directly compared, reasoning that—as both had a putative common pathology—those areas of hypometabolism that remained would more specifically underpin the cognitive deficits peculiar to PCA. Here, matching groups for severity may be problematic as different patient groups may fail on a given task for different reasons. In the present study, the two groups were matched by duration of symptoms, accepting that this too may be flawed if different variants of Alzheimer's disease follow different time trajectories.

The results of the PCA comparison with typical Alzheimer's disease showed a much more specific pattern of abnormality. Hypometabolism extending from the primary visual cortex through the dorsal visual association cortex to the parietal lobe, suggesting disruption to the dorsal stream of visual processing. This is precisely what would be predicted from the clinical data in the context of the two stream model of visual processing. Furthermore, the extension of the hypometabolic region to the right primary visual cortex is consistent with the finding of left visual hemifield defects on clinical examination. The marked asymmetry, with far greater right sided pathology, was, however, unexpected. Predominant left hemisphere hypometabolism has also been described in PCA,[18 21] as has symmetrical hypometabolism, such as that reported in the region of interest study of Pietrini *et al*.[22] It is difficult to explain this variability but it would seem likely to reflect differences in case selection in terms of the purity of visual impairment and the disease stage at which patients undergo scanning. In other words, bilateral or left side predominant cases may be more likely to show additional deficits such as aphasia. In this study, such cases were possibly excluded at recruitment, as their cognitive performance would not have been so selectively biased against visuospatial performance. Certainly the present group's left hemisphere was not spared (figs 2[f2] and 5[f5]), and it should be emphasised that the asymmetry was particularly related to the Alzheimer/PCA contrast. In other words, the right biased pathology in PCA (figs 4[f4] and 5[f5]) represented the abnormality this group had over and above that seen in typical Alzheimer's disease.

The only other statistical parametric mapping study of PCA, by Bokde *et al*,[23] also revealed symmetrical hypometabolism in posterior brain regions. Although primarily concerned with assessing partial volume effects, their results make an interesting contrast with the present study. The PCA group in that study was more demented than ours (mean (SD) MMSE, 16.8 (8.5) *v* 21.2 (5.1)) and it is possible that as cases become more advanced, left hemisphere involvement becomes more evident. Significantly, Bokde *et al*'s study did not include detailed neuropsychology and so it is not clear how ''pure'' the visuospatial deficits were in their cases. The other major difference between the two studies was that their field of view only extended to *z* +40 mm, so that the full

extent of fronto-parietal hypometabolism was not evaluated. This is not inconsequential, as it would have excluded some major abnormalities found in the present study such as the most significant statistical peak (z +58 mm, right parietal) and the frontal eye fields peaks ($z \geqslant 42$ mm). Finally, it should be noted that in contrast to Bokde *et al*, our statistical parametric mapping analysis did not include a partial volume correction, for the following reason. While differences in regional glucose metabolism between groups are less significant if the data are corrected for atrophy (which is greater in patient groups), it is likely that regional atrophy also contributes to the clinical profile. As the present study aimed to assess the regional neural correlates of a clinical syndrome, a partial volume correction was not implemented as it was felt that this may underestimate regional pathology by correcting for clinically significant atrophy. A partial volume correction was, however, used in the ROI study, as this analysis was concerned with providing absolute values of CMRglc in neural tissue.

The topography of the hypometabolic area remaining when PCA was contrasted with Alzheimer's disease (fig 4[f4]) is consistent with Hof *et al*'s hypothesis,[3] based on necropsy studies, that deficits in PCA arise because of disruption of long cortico-cortical pathways. They argued that, as neurofibrillary tangles (NFT) develop in the cell bodies of pyramidal neurones that form long cortico-cortical connections, Alzheimer's disease pathology causes disconnection of neocortical regions.[4] Studies in PCA have shown high NFT counts in layer III of BA 17, 18, and 19, suggesting that pathology at each of these points disrupts feed-forward dorsal stream pathways to BA 18, 19, and 7/23, respectively. On the other hand, a high density of neurofibrillary tangles in layers V and VI of BA 18 was proposed as evidence of damage to the feed-back projection to BA 17.[3 4] Based on the observation that senile plaques occur where the nerve terminals of neurones containing neurofibrillary tangles are degenerating,[38] Hof *et al* have also suggested that the distribution of senile plaques in PCA is consistent with the spread of pathology along this chain of connections.[4] The results of the present study offer in vivo support for this hypothesis, in that the pattern of hypometabolism (fig 4[f4]) appears very much consistent with dysfunction of a network of neurones extending from primary visual through visual association to parietal association cortex.

The comparison of PCA with controls also revealed bilateral regions of dorsolateral frontal hypometabolism (fig 2[f2], arrows, and fig 3[f3]) corresponding to the anatomical location of the frontal eye fields. The statistical parametric mapping contrast of PCA minus typical Alzheimer's disease did not show this abnormality at p(corrected) = 0.1 but this probably reflects insufficient power owing to the small size of the PCA group. When contrasted at a less rigorous statistical threshold (p(uncorrected) = 0.001), the hypometabolic region in the PCA group extended into the dorsolateral frontal lobe, sparing the more rostral prefrontal cortex.

The frontal eye fields are critical for the generation of normal voluntary eye movements, and receive significant inputs from dorsal visual association BA 18/19.[39] Functional imaging studies employing various paradigms to investigate saccadic eye movements in healthy volunteers have found activations in both dorsal stream (BA19 and 7) and frontal eye fields,[40–48] as have single unit electrophysiological recordings in animals.[49–51] There is controversy over the precise location of the frontal eye fields in humans. Although studies in non-human primates have implicated BA 8, functional activation studies in humans have generally shown more caudal activation (BA 6).[52] This issue was recently explored further by Lobel *et al* in a detailed study using both functional MRI (fMRI) and intracerebral electrical stimulation (IES).[53] They identified three regions with fMRI: a medial frontal area that was interpreted as supplementary eye field and two further areas which they called deep and lateral oculomotor areas (OMA). Of these three regions, the proposed frontal eye field clusters in the present study appear approximately equivalent to Lobel *et al*'s ''deep OMA''. They described this region as lying at the intersection of the superior frontal sulcus and the fundus of the superior precentral sulcus (left, $x = -24.5 \pm 4.9$, $y = -8.9 \pm 6.7$, $z = 49.8 \pm 4.2$, and right, $x = -22.6 \pm 3.7$, $y = 0.1 \pm 8.1$, $z = 52.2 \pm 4.1$). Furthermore, in their IES study, they reported that versive eye movements were most sensitively elicited by stimulation of the deep OMA compared with the other two regions. The Talairach coordinates of this IES site in the right hemisphere (left side not published) were $x = 26$, $y = 2$, $z = 46$. The peaks of the frontal eye field clusters in the present study lay slightly rostral to those of previous activation studies but they are overlapping. It is noteworthy that the coordinates for Lobel *et al*'s deep OMA IES site lies within the present right sided cluster. However, perhaps more compelling than the stereotaxic comparison is the observation that, when overlaid with MRI, the present clusters are located in the fundus of the caudal part of the superior frontal sulcus, consistent with previously published reports.[52 53]

As FDG-PET primarily measures synaptic activity,[54] we interpret frontal eye field hypometabolism as being caused by degeneration of the afferent input from the dorsal stream and propose that disruption of this pathway is the neural basis of ocular apraxia. Likewise, the ability to make accurate reaching movements to visually guided targets requires the visually derived spatial coordinates of the target to be passed from parietal to premotor areas. Disruption of neural connections between these areas—as would be expected from the PET findings in the PCA group—would, in addition, offer a plausible explanation for optic ataxia.

Conclusions

Our study showed that PCA is associated with a significant metabolic deficit, maximal in the occipito-parietal region. This finding is consistent with the prediction from the clinical profile that these deficits are primarily a result of disruption to the dorsal stream of visual processing. Hypometabolism in the frontal eye fields was also identified, suggesting an explanation for the ocular apraxia frequently seen in this syndrome. We propose that disruption of the dorsal stream is a consequence of the spread of pathology along a series of interconnected feed-forward and feed-back pathways. The key issue of why a minority of cases of Alzheimer's disease develop this atypical locus of pathology is at present unresolved.

Authors' affiliations

P J Nestor, J R Hodges, University of Cambridge, Neurology Unit, Addenbrooke's Hospital, Cambridge, UK
T D Fryer, Wolfson Brain Imaging Centre, University of Cambridge, Addenbrooke's Hospital
J Clarke, Department of Orthoptics, Addenbrooke's Hospital
D Caine, School of Psychology, University of Sydney, New South Wales, Australia

Competing interests: none declared

REFERENCES

1 **Benson DF**, Davis RJ, Snyder BD. Posterior cortical atrophy. *Arch Neurol* 1988;**45**:789–93.
2 **Hof PR**, Bouras C, Constantinidis J, *et al*. Selective disconnection of specific visual association pathways in cases of Alzheimer's disease presenting with Balint's syndrome. *J Neuropathol Exp Neurol* 1990;**49**:168–84.
3 **Hof PR**, Archin N, Osmand AP, *et al*. Posterior cortical atrophy in Alzheimer's disease: analysis of a new case and re-evaluation of a historical report. *Acta Neuropathol* 1993;**86**:215–23.

4 **Hof PR**, Vogt BA, Bouras C, *et al*. Atypical form of Alzheimer's disease with prominent posterior cortical atrophy: a review of lesion distribution and circuit disconnection in cortical visual pathways. *Vision Res* 1997;**37**:3609–25.
5 **Levine DN**, Lee JM, Fisher CM. The visual variant of Alzheimer's disease: a clinicopathologic case study. *Neurology* 1993;**43**:305–13.
6 **Galton CJ**, Patterson K, Xuereb JH, *et al*. Atypical and typical presentations of Alzheimer's disease: a clinical, neuropsychological, neuroimaging and pathological study of 13 cases. *Brain* 2000;**123**:484–98.
7 **Berthier ML**, Leiguarda R, Starkstein SE, *et al*. Alzheimer's disease in a patient with posterior cortical atrophy. *J Neurol Neurosurg Psychiatry* 1991;**54**:1110–11.
8 **Mackenzie Ross SJ**, Graham N, Stuart-Green L, *et al*. Progressive biparietal atrophy: an atypical presentation of Alzheimer's disease. *J Neurol Neurosurg Psychiatry* 1996;**61**:388–95.
9 **Hof PR**, Bouras C, Constantinidis J, *et al*. Balint's syndrome in Alzheimer's disease: specific disruption of the occipito-parietal visual pathway. *Brain Res* 1989;**493**:368–75.
10 **Victoroff J**, Ross GW, Benson DF, *et al*. Posterior cortical atrophy. Neuropathologic correlations. *Arch Neurol* 1994;**51**:269–74.
11 **Ala TA**, Frey WH, Clark HB. Posterior cortical atrophy: neuropathological correlations. *Arch Neurol* 1996;**53**:958.
12 **Pantel J**, Schroder J. Posterior cortical atrophy—a new dementia syndrome or a form of Alzheimer's disease? [[In German]]. *Fortschr Neurol Psychiatr* 1996;**64**:492–508.
13 **McKeith IG**, Galasko D, Kosaka K, *et al*. Consensus guidelines for the clinical and pathologic diagnosis of dementia with Lewy bodies (DLB): report of the consortium on DLB international workshop. *Neurology* 1996;**47**:1113–24.
14 **Hansen L**, Salmon D, Galasko D, *et al*. The Lewy body variant of Alzheimer's disease: a clinical and pathologic entity. *Neurology* 1990;**40**:1–8.
15 **Ungerleider LG**, Haxby JV. ''What'' and ''where'' in the human brain. *Curr Opin Neurobiol* 1994;**4**:157–65.
16 **Hof PR**, Bouras C. Object recognition deficit in Alzheimer's disease: possible disconnection of the occipito-temporal component of the visual system. *Neurosci Lett* 1991;**122**:53–6.
17 **Evans JJ**, Heggs AJ, Antoun N, *et al*. Progressive prosopagnosia associated with selective right temporal lobe atrophy. A new syndrome? *Brain* 1995;**118**:1–13.
18 **Freedman L**, Selchen DH, Black SE, *et al*. Posterior cortical dementia with alexia: neurobehavioural, MRI, and PET findings. *J Neurol Neurosurg Psychiatry* 1991;**54**:443–8.
19 **Mendez MF**, Cherrier MM. The evolution of alexia and simultanagnosia in posterior cortical atrophy. *Neuropsychiatry Neuropsychol Behav Neurol* 1998;**11**:76–82.
20 **Foster NL**, Chase TN, Fedio P, *et al*. Alzheimer's disease: focal cortical changes shown by positron emission tomography. *Neurology* 1983;**33**:961–5.
21 **Kiyosawa M**, Bosley TM, Chawluk J, *et al*. Alzheimer's disease with prominent visual symptoms: clinical and metabolic evaluation. *Ophthalmology* 1989;**96**:1077–86.
22 **Pietrini P**, Furey ML, Graff-Radford N, *et al*. Preferential metabolic involvement of visual cortical areas in a subtype of Alzheimer's disease: clinical implications. *Am J Psychiatry* 1996;**153**:1261–8.
23 **Bokde AL**, Pietrini P, Ibanez V, *et al*. The effect of brain atrophy on cerebral hypometabolism in the visual variant of Alzheimer disease. *Arch Neurol* 2001;**58**:480–6.
24 **Mendez MF**, Ghajarania M, Perryman KM. Posterior cortical atrophy: clinical characteristics and differences compared to Alzheimer's disease. *Dement Geriatr Cogn Disord* 2002;**14**:33–40.
25 **McKhann G**, Drachman D, Folstein M, *et al*. Clinical diagnosis of Alzheimer's disease. *Neurology* 1984;**34**:939–44.
26 **Folstein MF**, Folstein SE, McHugh PR. ''Mini-mental state''. A practical method for grading the mental state of patients for the clinician. *J Psychiatr Res* 1975;**12**:189–98.
27 **Wechsler DA**. *Wechsler memory scale – revised*, San Antonio: Psychological Corporation, 1987.
28 **Howard D**, Patterson K. *Pyramids and palm trees: a test of semantic access from pictures and words*. Bury St Edmunds: Thames Valley Publishing Company, 1992.
29 **Bozeat S**, Lambon Ralph MA, Patterson K, *et al*. Non-verbal semantic impairment in semantic dementia. *Neuropsychologia* 2000;**38**:1207–15.
30 **Warrington EK**, James M. *The visual object and space perception battery*. Bury St Edmunds: Thames Valley Test Company, 1991.
31 **Osterreith PA**. Le test de copie d'une figure complexe [[in French]]. *Arch Psychologie* 1944;**30**:206–56.
32 **Kinahan PE**, Rogers JG. Analytic 3D image reconstruction using all detected events. *IEEE Trans Nucl Sci* 1989;**36**:964–8.
33 **Phelps ME**, Huang SC, Hoffman EJ, *et al*. Tomographic measurement of local cerebral glucose metabolic rate in humans with (F-18)2-fluoro-2-deoxy-D-glucose: validation of method. *Ann Neurol* 1979;**6**:371–88.
34 **Ichimiya A**, Herholz K, Mielke R, *et al*. Difference of regional cerebral metabolic pattern between presenile and senile dementia of the Alzheimer type: a factor analytic study. *J Neurol Sci* 1994;**123**:11–17.
35 **Desgranges B**, Baron JC, de la Sayette V, *et al*. The neural substrates of memory systems impairment in Alzheimer's disease. A PET study of resting brain glucose utilization. *Brain* 1998;**121**:611–31.
36 **Talairach J**, Tournoux P. *Co-planar stereotaxic atlas of the human brain. 3-Dimensional proportional system: an approach to cerebral imaging*. Stuttgart: George Thieme Verlag, 1988.
37 **Meltzer CC**, Kinahan PE, Greer PJ, *et al*. Comparative evaluation of MR-based partial-volume correction schemes for PET. *J Nucl Med* 1999;**40**:2053–65.
38 **Hyman BT**, Van Hoesen GW, Kromer LJ, *et al*. Perforant pathway changes and the memory impairment of Alzheimer's disease. *Ann Neurol* 1986;**20**:472–81.
39 **Nieuwenhuys R**, Voogd J, van Huijzen C. *The human central nervous system: a synopsis and atlas*, 3rd Berlin: Springer-Verlag, 1988.
40 **Kimmig H**, Greenlee MW, Gondan M, *et al*. Relationship between saccadic eye movements and cortical activity as measured by fMRI: quantitative and qualitative aspects. *Exp Brain Res* 2001;**141**:184–94.
41 **Petit L**, Orssaud C, Tzourio N, *et al*. Functional anatomy of a prelearned sequence of horizontal saccades in humans. *J Neurosci* 1996;**16**:3714–26.
42 **Grosbras MH**, Leonards U, Lobel E, *et al*. Human cortical networks for new and familiar sequences of saccades. *Cereb Cortex* 2001;**11**:936–45.
43 **Darby DG**, Nobre AC, Thangaraj V, *et al*. Cortical activation in the human brain during lateral saccades using EPISTAR functional magnetic resonance imaging. *Neuroimage* 1996;**3**:53–62.
44 **Bodis-Wollner I**, Bucher SF, Seelos KC, *et al*. Functional MRI mapping of occipital and frontal cortical activity during voluntary and imagined saccades. *Neurology* 1997;**49**:416–20.
45 **Sweeney JA**, Mintun MA, Kwee S, *et al*. Positron emission tomography study of voluntary saccadic eye movements and spatial working memory. *J Neurophysiol* 1996;**75**:454–68.
46 **O'Driscoll GA**, Alpert NM, Matthysse SW, *et al*. Functional neuroanatomy of antisaccade eye movements investigated with positron emission tomography. *Proc Natl Acad Sci USA* 1995;**92**:925–9.
47 **Anderson TJ**, Jenkins IH, Brooks DJ, *et al*. Cortical control of saccades and fixation in man. A PET study. *Brain* 1994;**117**:1073–84.
48 **Doricchi F**, Perani D, Incoccia C, *et al*. Neural control of fast-regular saccades and antisaccades: an investigation using positron emission tomography. *Exp Brain Res* 1997;**116**:50–62.
49 **Gnadt JW**, Andersen RA. Memory related motor planning activity in posterior parietal cortex of macaque. *Exp Brain Res* 1988;**70**:216–20.
50 **Barash S**, Bracewell RM, Fogassi L, *et al*. Saccade-related activity in the lateral intraparietal area. II.Spatial properties. *J Neurophysiol* 1991;**66**:1109–24.
51 **Bruce CJ**, Goldberg ME, Bushnell MC, *et al*. Primate frontal eye fields. II.Physiological and anatomical correlates of electrically evoked eye movements. *J Neurophysiol* 1985;**54**:714–34.
52 **Paus T**. Location and function of the human frontal eye-field: a selective review. *Neuropsychologia* 1996;**34**:475–83.
53 **Lobel E**, Kahane P, Leonards U, *et al*. Localization of human frontal eye fields: anatomical and functional findings of functional magnetic resonance imaging and intracerebral electrical stimulation. *J Neurosurg* 2001;**95**:804–15.
54 **Kadekaro M**, Crane AM, Sokoloff L. Differential effects of electrical stimulation of sciatic nerve on metabolic activity in spinal cord and dorsal root ganglion in the rat. *Proc Natl Acad Sci USA* 1985;**82**:6010–13.